Researches on Substrates of High Temperature Eddy Current Sensor

Chao Han[a], Longxiang Xu[b],Yingzhe Lin[c]

[a] College of Mechanical and Electrical Engineering, Nanjing University of Aeronautics and Astronautics, Yudao St 29, B221 Nanjing, China, cold-wave777@163.com

[b] College of Mechanical and Electrical Engineering, Nanjing University of Aeronautics and Astronautics, Yudao St 29, B315 Nanjing, China, fqp@nuaa.edu.cn

[c] Nanjing CIGU Limited Corporation, Jiuzhu Rd 100, Nanjing, China, lyz@cigu.org.cn

***Abstract*—In this paper, substrates of eddy current sensor were composed by silver films and glass ceramic disks, all of these can resist high temperature. The thin silver films were deposited by radio frequency magnetron sputtering on machinable glass ceramic at room temperature. Variations of sputtering power, bios voltage and power density were carried out for each deposition, then parts of as-deposited samples were subjected to annealing at 600℃ within a vacuum chamber. Structural properties were studied by X-ray diffraction (XRD) and scanning electron microscope (SEM). It was shown that structural properties had a strong dependency on sputtering power and annealing temperature. Electrical contact resistance measured by a four point probe instrument was directly affected by the thickness of films. It was also found that the film conductivity, especially in thinner films, was improved by the increasing grain size. Further more, the film adhesion was observed by scratch tests experiment. Finally, the subsequent processes of high temperature eddy current sensor were introduced.**

1 Introduction

There is a general agreement in the literature that metal films are widely used as coatings in the field of electronics, meanly because their low resistivity, high-thermal conductivity and excellent ductility [1,2]. And their properties have been extensively studied, but few researches have been offered to the application of metal films in high temperature. Traditionally, some active metals (Cr, Cu, Ni) are used for coating films. But they are easily contaminated by oxygen in high temperature. On the contrary, some inert metals (Au, Pt) which show strong stability in high temperature are difficult to obtain [3]. Finally, considering about the performance in inertness and cost-effective, silver attracts specific interest of researchers in coating films.

Different technologies have been reported to produce silver films with adequate performances for application in electronic devices: physical vapor deposition (PVD), vacuum evaporation, vacuum winding coating, DC and radio frequency (RF) magnetron sputtering [4]. In this work, silver films are prepared by RF magnetron sputtering for its some advantages: high deposition rate, high power efficiency, low temperature and good performances in smoothness, uniformity and binding force.

The use of glass ceramic disks as substrates for deposition has several advantages: machinability makes it can be machined to be any shape, high temperature resistance makes it can be worked in high temperature environment and high thermal expansion coefficient ($8.7\times10^{-6}/℃$) generates small thermal stress between silver films and substrates under large temperature difference[5,6].

2 Experimental details

Magnetron sputtering deposition were done with the sputtering target of a 60mm diameter 99.99% purity pure silver disk to the substrates of the 3mm thickness and 10 mm diameter glass ceramic disks. Considering about the bond strength between silver films and substrates, the glass ceramic disks were slightly polished to the roughness Ra under 1 μm.

All the substrates were cleaned in an ultrasonic bath with acetone and dried before inserted into vacuum chamber. The distance between target and substrate was 50 mm. The working pressure in vacuum chamber could reach approximately 0.001 Pa due to the utilization of a turbo molecular-diaphragm pump combination.

The sputtering gas was filled with high-purity argon (99.99%) and the pressure was stably about 4 Pa. A gas flow controller was used to maintain the argon flow in the chamber at 10 SCCM.

Before film deposition, the target was pre-sputtered on the shield about 30 minutes to remove the contaminations in the target surface and stabilize the magnetron parameters. In the deposition, the performances of the silver films were determined by the magnetron parameters, such as the sputtering power, bias voltage, power density, deposition rate, deposition time, deposition thickness and annealing condition et al. therefore, the eight samples were distributed into four groups based on various magnetron parameters (as shown in Table 1).

TABLE I. SAMPLES WITH DIFFERENT PROCESSING PARAMETERS

Sample No.	Sputtering power (W)	Bias voltage (V)	Power density (W/cm2)	Deposition rate (nm/min)	Deposition time (min)	Deposition thickness (μm)	Annealing condition
a1	40	340	1.42	37	40	1.5	
a2							annealed
b1	100	525	3.54	50		2	
b2							annealed
c1	160	650	5.66	63		2.5	
c2							annealed
d1	250	820	8.85	125		5	
d2							annealed

The samples (a2,b2,c2,d2) we chose from each group were placed into a vacuum chamber which was then pumped to a pressure of 1.3 × 10-3 Pa and annealed stepwise at temperature of 600 °C to anneal with 30 minutes. After definite time intervals the annealing was interrupted, and after cooling to room temperature the chemical composition and crystal structure of all the films was analyzed by X-ray diffraction (XRD) D8 ADVANCE with Cu Kα radiation and parallel beam geometry with a 2° incidence angle. After that, the samples were cut apart and inlaid. Then, the inlaid samples were polished in order to observe the cross-section surface profile.

Moreover, the cross-section morphologies were observed by SEM. Considering about the non-conductivity of cross-section, the inlaid samples ware coated with 20nm gold in 4 minutes by sputter coater K550X EMITECH in order to add their conductivity.

Electrical resistivity of silver films was acquired at room temperature by four point probe instrument RG-7C from NAPSON Corporation. The thickness of films was also input into the four point probe instrument to ensure the accuracy. The contact force between probes and samples was detected and adjusted during measurement to avoid that the probes puncture thin films. This analysis delivered ρ values within an error margin of ~1%.

Finally, the film adhesion was measured by a micro scratch tester WS-2005. It is equipped with a standard diamond indenter with 120° taper angle and 0.2mm radius. During the measurement, a loading rate of 25N/min was used with scratches rate of 1mm/min. The critical load was detected by a force sensor within the micro scratch tester in rupture position of films to calculate the adhesive stress by equation (6), thereafter the scratches images were observed by SEM.

3 Results

3.1 X-ray diffraction

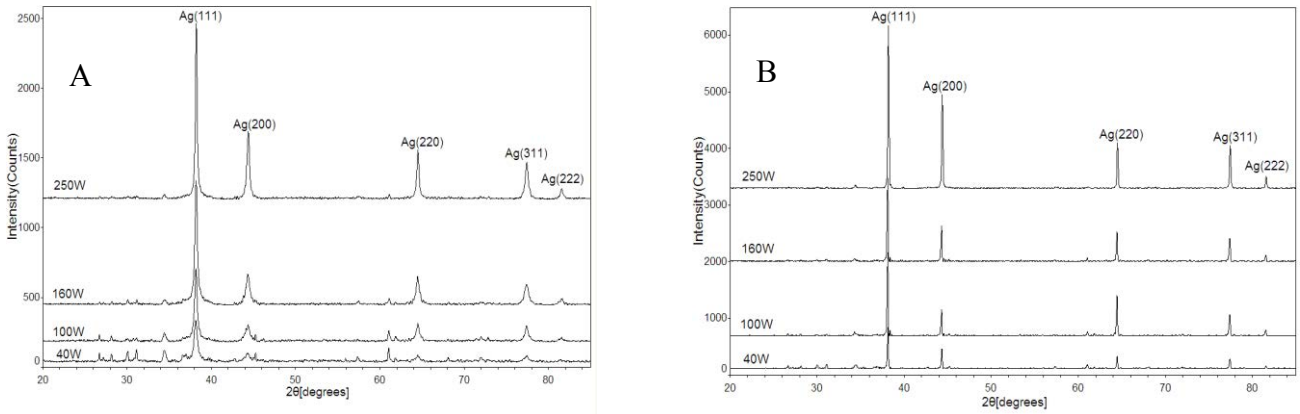

Figure.1. XRD patterns for: A) as-deposited silver films with different sputtering power, B) annealed silver films with different sputtering power

Fig.1 shows the XRD spectrums of the silver films for the various different sputtering powers and annealing conditions. In order to minimize the errors of the experiment, prior to the analysis of the XRD spectrums, the back ground was subtracted. After this process, the diffraction peaks are completely symmetric and without any background. As shown in fig.1, the peaks indicate the polycrystalline nature of the silver films. And the strongest diffraction in each sample is the Ag (111), which can be observed in each sample. In addition, the peak becomes sharper with the increasing of sputtering power, meanwhile the splitting of diffraction peaks decrease or even disappear.

From the FWHM of diffraction peak (111), the average grain diameter of silver films can be estimated by the Scherrer formula as [7]

$$d = \frac{k\lambda}{\beta \cos\theta} \tag{1}$$

where d is the grain size in the silver films, the Scherrer constant k is taken equal to 0.9, λ (0.15406nm) is the wavelength of the X-ray, β is the FWHM of peak (111) can be indicated from

Table 2, and θ (2θ=38.2°) is the diffraction angle of peak (111).

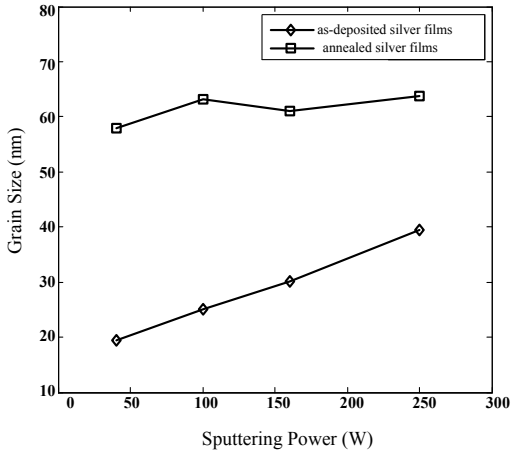

Figure.2. Grain size of silver films with different sputtering power and different annealing condition

Fig.2 shows that the grain size of films with the range form 19.4nm to 39.5nm for various sputtering power. And they steadily increase during annealing to about 60nm. With a higher growth rate, the initial silver crystals enlarge quickly before the nuclei are uniformly formed. And the grain sizes become larger after annealing due to the merging processes.

3.2 Microstructure

Fig.3 shows cross-sectional SEM images of two silver films with same sputtering power but different annealing condition. These two images show that the annealing process induce some changes in the morphological features of silver films. From the cross-section images with higher magnification (right column), one can clearly observe that silver aggregates have a significant change in size and shape, with diameters of grain varying from a few nanometers (as-deposited sample) to about 60nm (annealed sample).

The reason to believe that this suggestion is true is the result of work by K. Heinemann and H. Poppa [8] in which direct evidence is reported for the simultaneous occurrence of Ostwald ripening and short distance cluster mobility during annealing of silver films onto MGC surfaces in the temperature about 600°C. And this is confirmed by the variation of grain size detected by XRD shown in Fig.2.

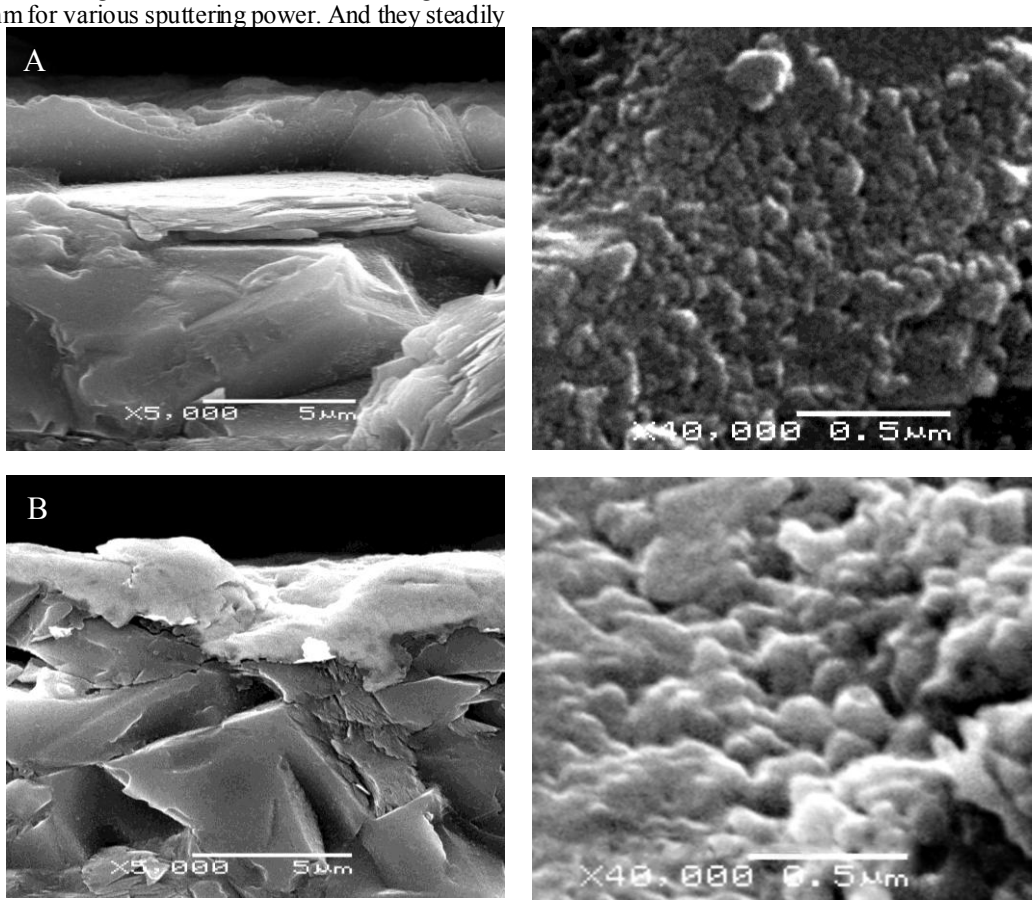

Figure 3. Fractured cross-section SEM images of two silver films with different annealing condition: (A) 160 W, (B) 160 W and annealed. The images in the right column are the same films taken at a higher magnification.

3.3 Electrical properties

The electrical resistivity of the different films at room temperature was measured by four probe measurements. The numerical value ρ_0 showed in instrument is calculated by the following equation [9],

$$\rho_0 = 2\pi S \frac{V}{I} \quad (2)$$

Where S is the distance between two adjacent probes, V is the potential difference between two inside probes, and I is the current flowing thought two outside probes. ρ_0 can be considered to be electrical resistivity ρ theoretically, if the distance between test point and border of films is greater than 4S. In this experiment, the condition of distance is not met. So the modifying factor B_0 should be taken in consideration, and electrical resistivity ρ should be written as

$$\rho = \frac{\rho_0}{B_0} = 2\pi S \frac{V}{I} \cdot \frac{1}{B_0} \quad (3)$$

The electrical resistivity ρ of silver films with different thickness and annealing condition after correction is showed in Fig. 4.

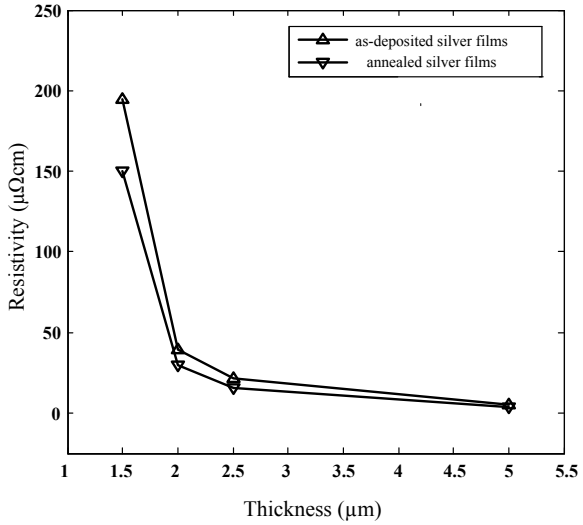

Fig.4. Electrical resistivity as a function of the thickness of silver films with different annealing condition

From Fig.4 one may notice that silver films at thickness of 1.5 μm exhibit higher resistance values (about 200 $\mu\Omega cm$) than that of others and this can explain the fact that the silver films at the lowest sputtering power exhibit darker images which showed in Fig3. When the film thickness increases to 2 μm, the ρ value decreases dramatically to about 40 $\mu\Omega cm$. When the film thickness further increases about 5 μm, the ρ value reaches about 3 $\mu\Omega cm$, being almost the same as that of bulk Ag (1.6 $\mu\Omega cm$). So a conclusion can be made that the electrical resistivity is directly affected by the thickness of films.

One may also notice that, the ρ value of silver films at thickness of 1.5 μm is lower after the annealing treatment than they have been before it, falling from 196 $\mu\Omega cm$ to 150 $\mu\Omega cm$. This is due to the fact that the increasing crystal grain size caused by annealing treatment decreases the grain boundary scattering of electrons [10,11].

3.4 Scratch tests

Scratch tests of silver films were carried out for with a loading rate of 25N/min. Fig.5A shows the total scratch track of film for an increasing load from 0 to 100N in 4 minutes. It is obvious that the width of scratch track is broadened with the increasing of load [12]. Fig.5B shows the scratch track in the rupture position. Where, the contact force added up to the critical load and the delaminating between film and substrate occurred.

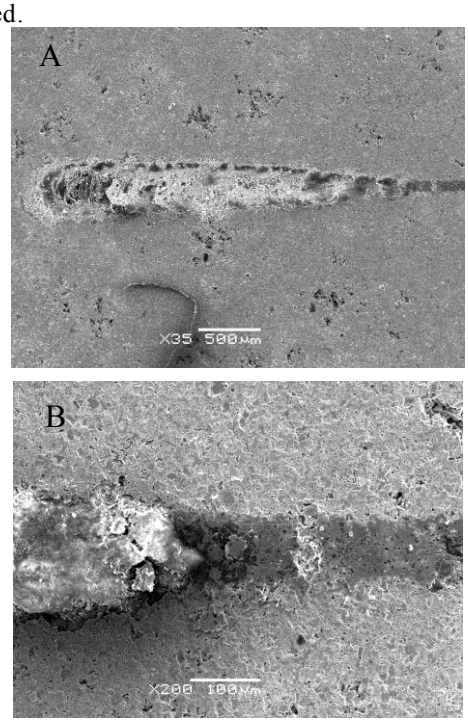

Figure 5. SEM images of scratch tests for silver films: (A) scratch track of film with an increasing load from 0 to 100N, (B) scratch track of film in rupture position

The critical load for all films shows the similar value about 30N. It can be deduced that what directly affects the critical load are not the film thickness and annealing condition but the property of substrate and coating technique.

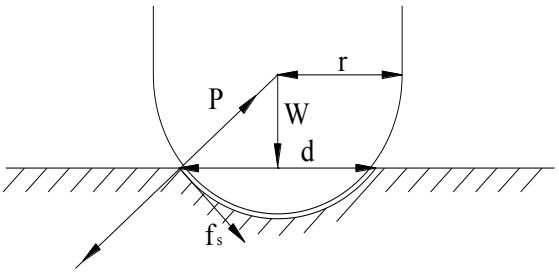

Figure.6. Schematic diagram of relationship between force and deformation of film

Fig.6 shows the relationship between force and deformation of film in the scratch tests. Where r is the radius of indenter with 0.2mm, W is the contact force given by indenter, d is the width of scratch track which can be measured from Fig.5, P is the resistance given by substrate, which can be expressed as [13]

$$P = \frac{W}{\pi d^2} \tag{4}$$

And f_S is shear press of film which can be calculated by the following equation,

$$f_S = \sqrt{\frac{W}{\pi r^2 P - W}} \cdot P \tag{5}$$

When contact force (W) equals to the critical load (W_C), the critical value of f_S can be considered as the adhesive stress and it should be equal to

$$f_{SC} = \sqrt{\frac{W_C}{\pi r^2 P - W_C}} \cdot P \tag{6}$$

According to equation (6), the range of critical values (f_{SC}) is calculated to be 245 N/mm^2 . Comparing with the traditional methods such as electroplating and directing bonding (80 N/mm^2), the films deposited by RF magnetron sputtering shows a better performance due to the excellent penetrating power of high kinetic energy silver atoms.

4 Subsequent processes

The silver films made by radio frequency magnetron sputtering have good performance in structure, conductivity and adhesion. They are ideal material for metallizing of glass ceramic. Because of the conductivity of continuous silver films, the films cannot be used for micro electroforming directly. So lithograph and thin film etching is necessary. The process contains for parts: depositing of positive photoresist, exposure, development and etching of silver film. After that, the silver films after etching have ideal pattern and the second lithograph will be performed for micro electroforming. The process contains depositing of negative photoresist, exposure and development. After that, the silver films after etching expose for conductivity layer and micro electroforming can be performed.

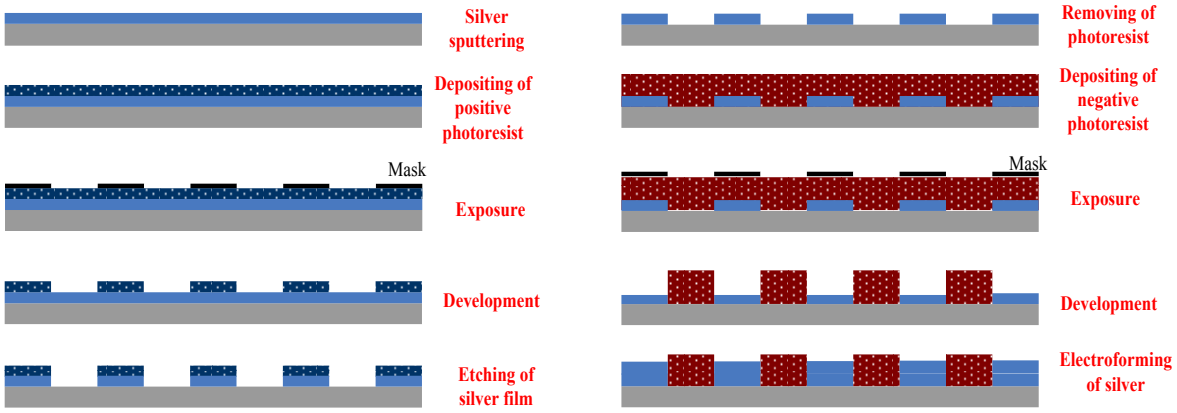

Figure 7. The subsequent processes of high temperatureeddy current sensor

5 Conclusions

In this paper, thin silver films were deposited on the glass ceramic by RF magnetron sputtering at room temperature. As a result, the deposition rate rises from 50nm/min to 125nm/min with the increasing of the sputtering power.

After that, annealing treatments at 600℃ were carried out on parts of as-deposited samples. And the microstructure, the topography, the electrical properties and the adhesive stress of films were investigated by X-ray diffraction, scanning electron microscope, four point probe instrument and micro scratch tester respectively.

The experimental results show that the increase of sputtering power will increase the grain size as well as the surface roughness. In addition, due to the annealing treatments, the grain size is increased further, whereas, the surface roughness is dropped.

For thicker films (5 μm), deposition at 250W led to a low value of the resistivity (3 $\mu\Omega cm$) compared to that of bulk Ag (1.6 $\mu\Omega cm$). Annealing treatment reduced the

resistivity due to the increasing of crystal grain size. But, the observed changes of conductivity were meanly attributed to differences in the film thickness and the surface topography. And, the adhesive stress deposited by RF magnetron sputtering reached 245 N/mm^2, which shows a significant improvement than traditional methods.

Finally, the subsequent processes were introduced briefly. They contained two lithography, thin film etching and micro electroforming. These processes ensured the manufacture of silver coils on glass ceramic.

REFERENCES

[1] T. Suzuki, Y. Abe, M. Kawamura, et al. Optical and electrical properties of pure Ag and Ag-based alloy thin films prepared by RF magnetron sputtering [J]. Vacuum, 2002, 66: 501-504.

[2] K. Sarakinos, J. Wördenweber, F. Uslu, et al. The effect of the microstructure and the surface topography on the electrical properties of thin Ag films deposited by high power pulsed magnetron sputtering [J]. Surf. Coat. Technol, 2008, 202: 2323-2327.

[3] R.C. Adochite, D. Munteanu, M. Torrell, et al. The influence of annealing treaments on the properties of Ag:TiO2 nanocomposite films prepared by magnetron sputtering [J]. Surf. Sci, 2012, 258: 4028-4034.

[4] P.G. Kelly, R.D. Arnell. Magnetron sputtering: a review of recent developments and applications [J]. Vacuum, 2000, 56:159-172.

[5] S. Voss, S. Gandikota, R. Tao, et al. Adhesion studies of CVD copper metallization [J]. Microelectronic Eng, 2000, 50:501-508.

[6] N. Iwase, A. Tsuge, Y. Sugiura. Development of a thermal conductive AIN ceramic substrate technology [J]. Hybrid Microelectron, 1984, 7:49-53.

[7] L. Duan, X. Yu, L. Ni, Z. Wang. ZnO:Ag film growth on Si substrate with ZnO buffer layer by rf sputtering [J]. Appl. Surf. Sci, 2011, 257: 3463-3467.

[8] L.F. Senna, C.A. Achete, T. Hirsch, et al. Structural, chemical, mechanical and corrosion resistance characterization of TiCN coatings prepared by magnetron sputtering [J]. Surf. Coat. Technol, 1997, 94-95: 390-397.

[9] H.B. Wang, Z.Q. Wu. Advocating the physical experiment method [M]. Higher Education Press, 1990.

[10] D.M. Sun, Z.Q. Sun. Metal ceramic film and its applications in photoelectron technology [M]. Science Press, Beijing, 2004.

[11] N. Nedfors, O. Tengstrand, E. Lewin, et al. Structural, mechanical and electrical-contact properties of nanocrystalline-NbC/amorphous-C coatings deposited by magnetron sputtering [J]. Surf. Coat. Technol, 2011, 206: 354-359.

[12] M. Jing, R.L. Fu, H. He, et al. Direct bonded metal substrates and bonding methods [J]. Aerospace Materials and Technology, 2008, 3:1-7.

[13] D.Q. Xiao, J.G. Zhu, J.L. Zhu, et al. Film physics and device [M]. National Defense Industry Press, Beijing, 2011.